Timber strong-backs as cost-effective seismic retrofit method for URM buildings

M. Giaretton, J.M. Ingham & D. Dizhur

Department of Civil and Environmental Engineering, University of Auckland, Auckland

2017 NZSEE Conference

ABSTRACT: Out-of-plane failures induced by earthquake loads are one of the most critical deficiencies of clay brick unreinforced masonry (URM) buildings. Despite a number of seismic improvement techniques having been previously investigated and applied, there is a significant lack of experimentally validated solutions that consider the viability of these interventions in terms of overall associated cost and practicality, and impact on the building tenants, aesthetics and heritage building fabric. The main objectives of the research presented herein were to develop and validate seismic securing techniques for URM walls that satisfied the above conditions, in consultation with industry representatives. Full-scale shake-table testing of two cavity and three double-leaf solid clay brick URM walls was undertaken. The vertical timber framing that is typically a non-structural support of the inner wall lining was used as part of the retrofit solution and was fixed to the wall with steel brackets and mechanical screw-ties in order to form a strong-back. Wall and retrofit construction details, test set-up, observed crack-patterns, peak ground acceleration (PGA), wall acceleration and displacement profiles at failure, and quantification of the improvement in seismic capacity associated with use of the proposed retrofit technique are presented herein.

1 INTRODUCTION

A URM wall subjected to out-of-plane loading can be idealized as a one-way vertically spanning strip with a horizontal crack at some height within the span (Penner and Elwood 2016). There are two basic failure modes in which out-of-plane failure occurs: cantilever failure and beam type failure. The determining factor between which failure mode occurs is the adequacy of the anchorage at the floor and roof connections (Russell 2010). When connections to the diaphragm are inadequate, the wall becomes a tall unrestrained cantilever and results in collapse when the inertial force of the wall push it beyond its point of static instability. If the anchorage to the diaphragm is adequate, the wall will fail in 'beam type failure' and cracking occurs above mid-height leading to rocking of the two parts as two separate rigid bodies. The inertial forces on the wall are distributed to the diaphragm, causing the wall to act in bending and being reliant on the limited tensile strength of the mortar (Meisl 2007). Out-of-plane beam-type failure can either occur in one-way bending or two-way bending. One-way bending tends to occur in longer walls or walls without side supports whereas two-way bending requires the support of at least one vertical edge (Dizhur et al. 2014). Factors effecting the response of the wall include (Penner and Elwood 2016): the height to thickness ratio of the wall, weight carried by the wall, quality of mortar and construction, strength and stiffness of diaphragm and displacement response of the structure.

One method for the out-of-plane seismic retrofit of URM walls it to connect a series of vertical members (termed herein as strong-backs) to the interior surface of the wall (see **Figure 1**) at sufficient spacing to ensure that the width of wall between supports is capable of resisting the out-of-plane forces. Strong-backs act in flexure in order to transfer wall loads to the adjacent floor diaphragms, breaking up a large planar wall into a number of buttressed segments. A similar approach was proposed by (King 2009) using strong-backs as a retrofit strategy to protect masonry cladding structures from blast loading. Strong-back members are connected to the URM material via adhesive anchors or through-plate anchors, which allows a high level of reversibility should the need to remove the retrofit system arise. Design considerations when using strong-backs include height to thickness of a URM wall and spacing of strong-backs. The demand and capacity of the wall will dictate the spacing of the anchorages between the URM wall and strong-backs as well as the considerations of connection detailing to transfer loads into the diaphragm (FEMA 2006).

The shake-table experimental campaigns reported herein were conceived in order to investigate the performance of timber strong-backs applied to clay brick URM cavity- and solid- walls as a cost-effective seismic securing solution. The choice of using timber as a retrofit material comes from investigations of existing URM buildings in New Zealand that showed that a large portion of these buildings had timber framing lined with plasterboard as the interior finish. Hence, validating a securing solution that connected the masonry to the timber framing as a load path into the diaphragm would provide a practical and low-cost seismic securing method. The idea refers also to the timber framing used as an earthquake-resistant system for masonry buildings during the Minoan era (Tsakanika-Theohari 2008) and later extended to the entire Mediterranean area (Ruggieri 2015).

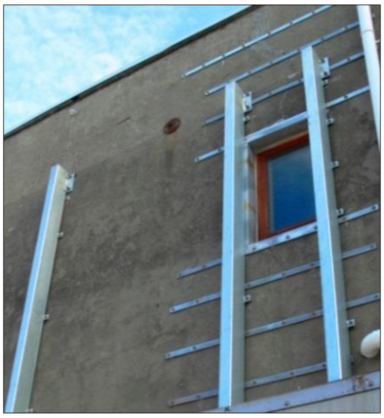

(a) External vertical steel strong-backs

(b) Internal vertical steel strong-backs

Figure 1. Examples of steel members used as strong-backs for out-of-plane retrofit of URM walls

2 TIMBER STRONG-BACK RETROFIT SOLUTION

The vertical strong-backs consist of 90 x 45 mm standard timber studs located at 550 mm spacings and secured to the URM wall using Ø12/230L mm mechanical screws, see **Figure 2**. This retrofit solution was investigated herein for application in both clay brick URM cavity- (see **Figure 3**) and solid-walls (see **Figure 2d,f,g**) with the aim of being a multi-purpose seismic mitigation system and as support to the inner wall lining as well as allowing space for the installation of electrical and plumbing systems.

Based on previous airbag testing of cavity-walls (Walsh et al. 2015), Ø12/230L mm mechanical screw were identified as the most effective retrofit solution in terms of increased out-of-plane cavity-wall capacity when compared with stainless steel helical rods and chemical ties. The screws had a hexagonal washer type head and a total threaded length of 160 mm as shown in **Figure 2e**, and were installed with a spanner in a pre-drilled Ø12 mm hole. The masonry was drilled using a low-impact drill making sure to limit vibrations in the walls, see **Figure 2a**. High torque is required during installation of Ø12 mm screw and from pull-out testing it was observed that in the case of weak bricks in lime-based mortar the screws had a tendency to split the bricks, resulting in a lower pull-out capacity of 18 kN (6 samples, COV 4%). In the cavity-walls the Ø12 mm mechanical screw also serves as a tie to secure the two wall leaves together (see **Figure 2b**) and hence the vertical timber studs were fixed using steel angle brackets mounted onto the wall at a spacing of 400 mm through the screws, see **Figure 2c** and **Figure 3**. In this way the screws reached at least half the depth of the bricks of the opposing masonry leaf (**Figure 3a**), thereby ensuring an adequate embedment length without modifying the external appearance of the building. In the solid-walls the screws were located at the centre of the timber studs with a vertical spacing of approximately 500 mm (see **Figure 4**) and using a washer countersunk 10 mm into the strong-back to provide a smooth surface for the wall lining, see **Figure 2d**. The base of the strong-backs was fixed to the floor-diaphragm (shake-table) using a 5 mm thick steel bracket and two Ø12 mm standard timber screws to allow the transfer of shear induced in the strong-back, see **Figure 2f**. The top of the strong-back was fixed to the roof-diaphragm using steel brackets and 30 mm long Ø5.5 mm standard timber screws, see **Figure 2c-d**. Standard GIB plasterboard was fixed to the timber strong-backs to demonstrate the aesthetic finish achievable using the securing technique, as shown in **Figure 2g**.

(a) Hole drilling (b) Cavity view of the final installation (c) Finish for cavity-wall

(e) Mechanical screws

(d) Finish for solid-wall (f) 5 mm steel brackets fixing base of strong-backs (g) Plasterboard finish

Figure 2. Installation process for timber strong-back retrofit

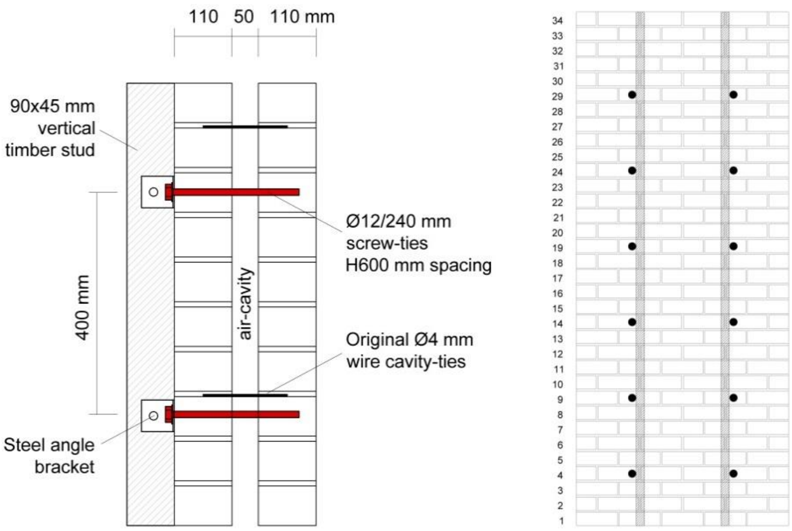

(a) Cross-section schematic (b) Screw spacing arrangement

Figure 3. Schematics of the timber strong-back retrofit technique applied to cavity-walls

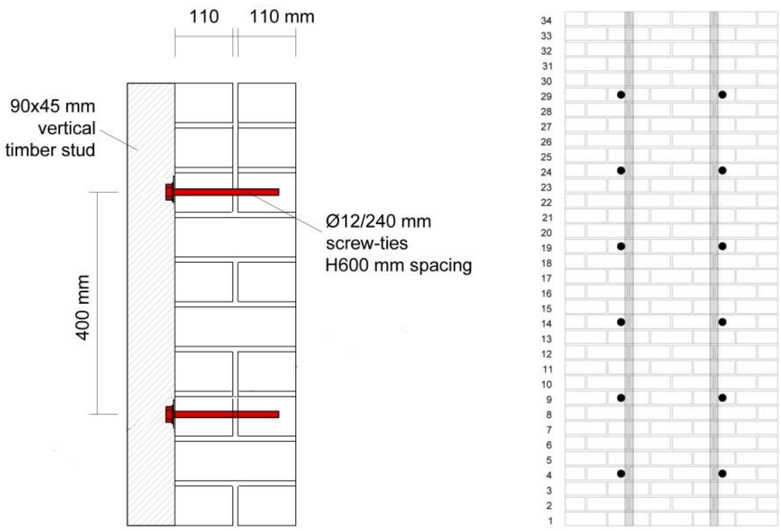

(a) Cross-section schematic (b) Screw spacing arrangement

Figure 4. Schematics of the timber strong-back retrofit technique applied to solid-walls

3 EXPERIMENTAL VALIDATON

3.1 Test programme and set-up

The strong-back retrofit technique was validated during two experimental shake-table campaigns: one focusing on cavity-walls (Giaretton et al. 2016b) and the second focused on the performance of solid-walls. Two tests were undertaken for cavity-walls in order to consider both as-built (W1) and retrofitted (W5) conditions. The retrofit was undertaken using vertical 90 x 45 mm standard timber studs @ approximately 600 mm horizontal spacings and secured with Ø12/230L mm mechanical screws @ 400 mm vertical spacing. Five tests were performed on solid-walls: (i) as-built condition, URM-p, with the parapet being secured in order to identify the response of the wall and avoid premature failure of the URM parapet, (ii) installing 90 × 45 mm timber strong-backs with mechanical screws @ 500 mm vertical spacing and securing the parapet, 45SB-p, (iii) using 90 × 90 mm timber strong-backs and mechanical screws applied in three different configurations. The three configurations were: (i) 90SB, wall strong-backs and as-built parapet, (ii) 90SB-p1, wall strong-backs and parapet secured only on the top and inner side (version 1), (iii) 90SB-p2, eccentric wall strong-back and parapet secured on the top and both inner and outer sides (version 2). **Table 1** summarises the characteristics of the tested walls including schematics and photos of each retrofit configuration.

The test set-ups were designed to replicate common in-situ boundary conditions for a single-story wall portion located at the top floor of a perimeter load-bearing URM wall, fixed at the base for continuity with the lower walls or foundation and allowing rotation and vertical displacement at the top based on typical seating arrangements observed at the roof level. During cavity-wall testing, the top wall restraint consisted of horizontal beams applied to both sides of the wall and into the air-cavity, see **Figure 5a**. Conversely, solid-walls were restrained at the top to simulate a timber diaphragm anchored to the wall using Ø12/230L mm mechanical screws and 50 mm square washers and composed of four 1500 mm lengths of 190 x 45 mm timber joists, see **Figure 5b**. For both test set-ups the top restraint was fixed to the purpose built protection frame and the base of the wall panel was secured with strong mortar between two stiff steel angles to prevent lateral movement of the wall base.

Accelerometers were installed at the bottom, middle, and top of the wall and on the shake-table (denoted as ACC B, ACC M, ACC T, and ACC ST in **Figure 5**), and three string potentiometers were attached at the middle and top of the wall and on the shake-table to measure differential displacement of the wall (denoted as DW M, DW T, and DW ST in **Figure 5**). Two additional accelerometers were mounted on the solid-wall at three quarter-height and onto the parapet. A single-axis acceleration-controlled sinusoidal test transitioning from 0.5 Hz to 50 Hz was applied with increasing acceleration of approximately 0.05g every 15 seconds and constant amplitude at 50 mm. All walls were tested until displaying signs of instability and within the range of the maximum possible load generated by the shake-table.

Table 1. Test matrix

	Wall	Securing Type	Spacing (mm)	Schematic	Photo example
CAVITY-WALLS	W1	URM (with original wire ties)	-	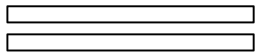	
	W5	2 x (90 x 45 mm) timber strong-back	600	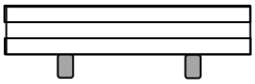	
SOLID-WALLS	URM-p	URM + parapet securing	-		
	45SB-p	2 x (90 x 45 mm) timber strong-back + parapet securing	600	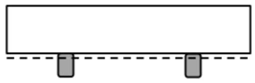	
	90SB	2 x (90 x 90 mm) timber strong-back (URM parapet)	600	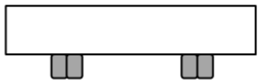	
	90SB-p1	2 x (90 x 90 mm)timber strong-back + parapet securing	600	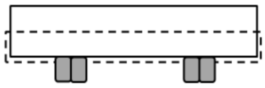	
	90SB-p2	1 x (90 x 90 mm) timber strong-back + parapet securing	1200	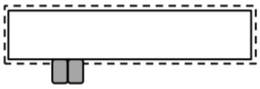	

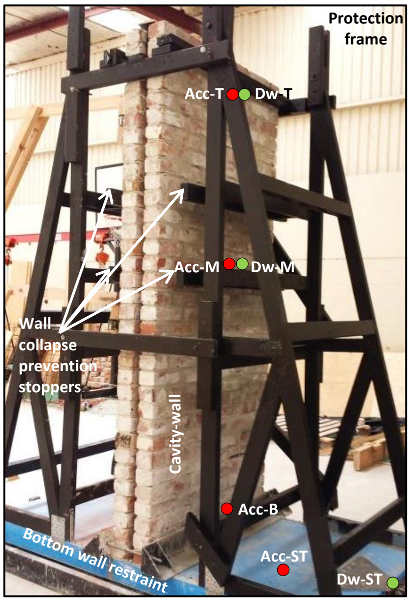

(a) Cavity-wall

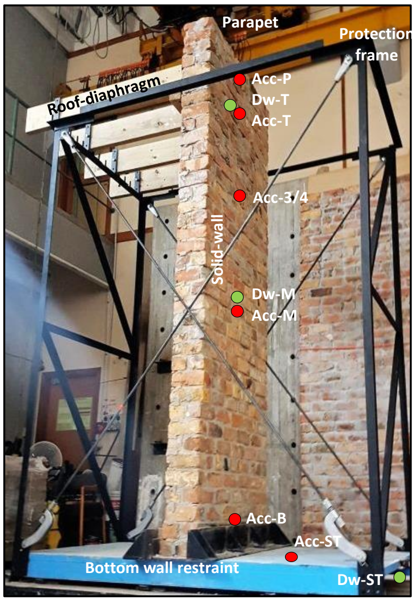

(b) Solid-wall

Figure 5. Test set-ups

3.2 **Wall characteristics**

The most commonly encountered boundary condition, geometric characteristics, and material properties for URM cavity-wall (Giaretton et al. 2016a) and solid-wall (Russell and Ingham 2010) arrangements were selected, and four walls that closely mimicked in-situ conditions were constructed using recycled clay bricks obtained from demolished vintage URM buildings. Brick dimensions were of size (230L × 110W × 75H mm) and compressive strength of 26.4 MPa (10 samples, COV 22%) for cavity-walls and 30.5 MPa (6 samples, COV 27%) for solid-walls, estimated using the half brick compression test (ASTM 2016a). The compressive strength of masonry prisms was 7.4 MPa (3 samples, COV 16%) and 8.2 MPa (3 samples, COV 20%) respectively, in accordance with (ASTM 2016b). The mortar mix was made from sand and lime in the ratio of 3:1 by volume respectively. 50 ×50 ×50 mm mortar test cubes were prepared during wall construction and were tested in compression after 28 days to obtain an average compressive strength of 0.54 MPa (6 samples, COV 18%, (ASTM 2013).

Test cavity-walls were constructed with two single URM leaves in a running bond pattern with a mortar joint thickness of approximately 10 to 15 mm. Masonry leaves were interconnected using 4 mm diameter horse-toe metal wire cavity-ties to replicate as-built field conditions (Giaretton et al. 2016b) (Giaretton, Dizhur, and Ingham 2016). Notches were cut into the wire near the outer-leaf to simulate the rusted and deteriorated condition of typical wire cavity-ties. Wire cavity-ties were laid based on the most common tie arrangement observed during preliminary surveys (Giaretton et al. 2016a), being two ties per row (600 mm) and one row of ties for every six masonry courses (450 mm). Cavity-wall samples were 3000 mm high, 1190 mm wide, and 270 mm thick including a 50 mm air-cavity.

Solid-wall test samples were two-leaf-thick common brick pattern walls with a mortar joint thickness of approximately 10–15 mm. The panels were 3300 mm high including a 300 mm high parapet above, and were 1200 mm wide and 230 mm thick.

3.3 **Dynamic response**

For all tests, cracking was mainly concentrated in the top quarter of the wall height (see **Figure 6**). As-built cavity-wall W1 exhibited differential movement of the two wall leaves, resulting in bending of the original cavity-ties and significantly reduced air-cavity width, see **Figure 6a**. The rocking capacity was influenced by mortar strength, with ultra-weak mortar tending to crumble, thereby reducing the contact area at the point of rotation and expediting rocking and, consequently, wall failure which occurred at 0.45g, see **Table 2**. The maximum displacement registered was 26 mm at mid-height and 17 mm at the top, see **Figure 7a**.

The use of 90 x 45 mm strong-backs in W5 significantly reduced the lateral mid-height displacement during testing, preventing the occurrence of both failure from rocking due to flexural tensile crack formation and out-of-plane bed-joint shear failure. The increased capacity resulted in the initiation of stiff global flexural behaviour at high levels of table acceleration (1.31g, see **Figure 6b** and **Table 2**) without reaching instability or collapse within the range of the maximum possible load generated by the shaking table. W5 exhibited a displacement profile comparable to W1, with 31 mm at mid-height and 13 mm at top (see **Figure 7a**), but at an acceleration that was three times higher than for W1.

As-built solid-wall URM-p displayed a typical one-way bending out-of-plane failure with major cracking at three quarter-height and minor cracking at mid-height (see **Figure 6c**). The formation of the three quarter-height crack caused a hinge effect, with the wall parts above and below beginning to rock as two separate almost-rigid bodies, inducing a large increase in acceleration at this level. As the three quarter-height displacement increased the flexural capacity of the wall was exceeded, causing the wall to collapse at 0.46g. The maximum displacement recorded near-collapse was 55 mm at top and 186 mm at mid-height, see **Figure 7b**.

45SB-p was retrofitted using 90 x 45 mm timber strong-backs from wall base to parapet top. Cracking and consequent falling of bricks occurred at the parapet edges, external to the strong-backs, as shown in **Figure 6d**. With increasing motion intensity a flexural behaviour was observed, leading to crack formation at three quarter-height followed by bricks being expelled from the surrounding area which involved only the outer leaf. The acceleration reached 1.33g, which was three times higher than that for the as-built condition. The displacement profile was linear, with 34 mm being recorded at top and 23 mm at mid-height, see **Figure 7b**, corresponding to a reduction with respect to the as built condition of 39% and 87% respectively.

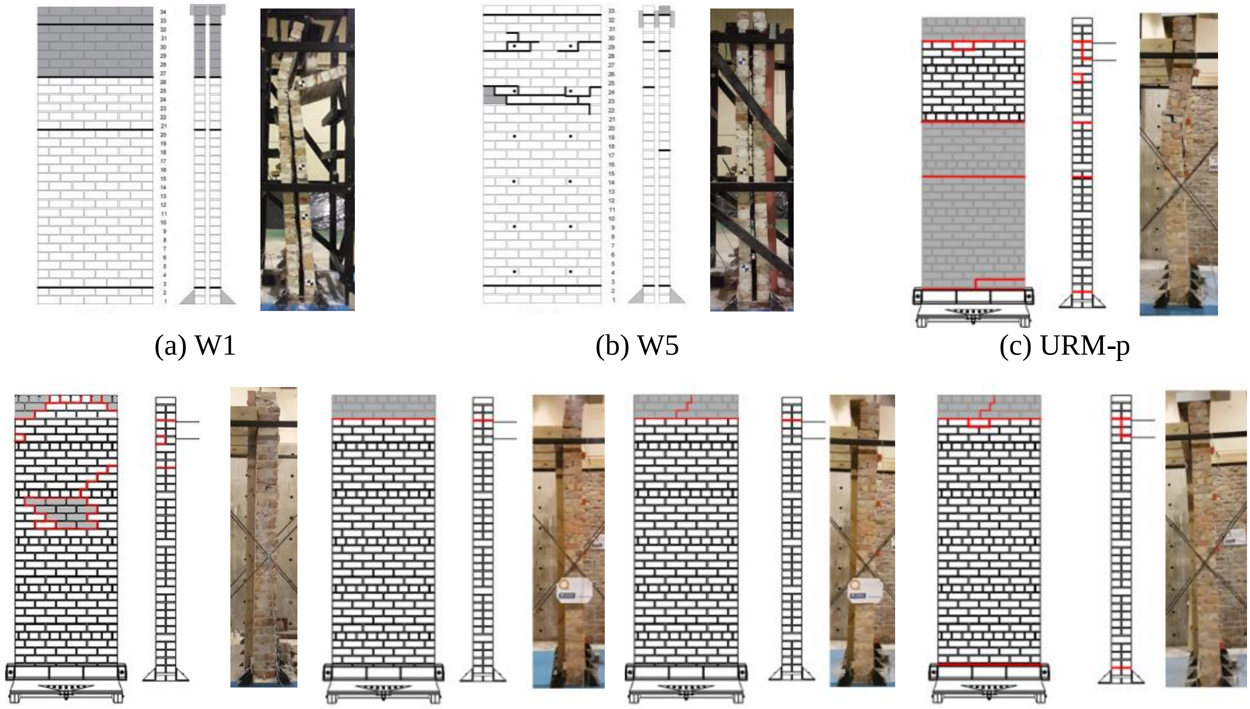

(a) W1 (b) W5 (c) URM-p

(d) 45SB-p (e) 90SB (f) 90SB-p1 (g) 90SB-p2

Figure 6. Screenshots showing crack-pattern survey and failure progression

Walls 90SB and 90SB-p1 were both retrofitted using 90 x 90 mm timber strong-backs, with the parapet being un-retrofitted in 90SB and being retrofitted in 90SB-p1. The linear displacement profile in **Figure 7b** clearly shows that the 90 x 90 mm timber strong-backs significantly increased the wall monolithic behaviour and prevented any cracks from forming. In wall 90SB the un-retrofitted parapet exhibited rigid-body rocking behaviour after cracking formed at the roof diaphragm level (parapet base), see **Figure 6e**. In wall 90SB-p1 the parapet was retrofitted with strong-backs and a single-side horizontal top restraint, preventing rocking failure but allowing the parapet to slide outwards on the existing cracking plane as motion intensity increased, see **Figure 6f**. 90SB and 90SB-p1 behaved similarly in terms of acceleration and displacement along the wall height (see profiles in **Figure 7b**). Instability due to parapet rocking or sliding was reached at approximately 0.96g (average value), corresponding to a maximum displacement of approximately 15 mm at mid-height and 23 mm at top. The recorded PGA was twice the value reached in the as-built condition and the reduction in displacement was 85% at mid-height and 77% at top. In wall 90SB-p2 the eccentricity caused by the strong-back position increased the stiffness of one end of the wall configuration in comparison to the other end, resulting in the initiation of torsion. A crack formed at the wall base, starting from the side without strong-backs and eventually propagated all the way through the base as the shake-table accelerations increased, see **Figure 6g**. The crack at the base allowed rocking to develop in the whole wall, which led to an increase in the displacement at the roof diaphragm level. The ultra-weak mortar did not provide enough friction against the increasing displacement, enabling brick pull-out where the mechanical screws were tied and resulting in the formation of a 15 mm gap between the wall and the roof diaphragm. Consequently the displacements registered were approximately twice those experienced by 90SB and 90SB-p1, even though the PGA was lower (0.82g, see **Table 2**). The single strong-back provided a sufficient increase in stiffness to prevent any cracks developing at the three quarter-height and mid-height, hence providing securing from out-of-plane failure. The parapet had a double-sided horizontal top restraint and hence did not present further damage.

Table 2: Summary of results

Wall ID	PGA		Max mid-height displacement		Max top displacement		Failure mode
W1	0.45g	(-)	26 mm	(-)	17 mm	(-)	One-way bending
W5	1.31 g	(291%)	31 mm	(119%)	13 mm	(76%)	Flexural behaviour
URM-p	0.46 g	(-)	186 mm	(-)	55 mm	(-)	One-way bending
45SB-p	1.33 g	(289%)	23 mm	(13%)	34 mm	(61%)	Flexural behaviour
90SB	0.95 g	(205%)	14 mm	(7%)	20 mm	(36%)	Rigid body behaviour and parapet rocking
90SB-p1	0.97 g	(209%)	15 mm	(8%)	25 mm	(46%)	Rigid body behaviour and parapet sliding
90SB-p2	0.82 g	(177%)	28 mm	(15%)	38 mm	(69%)	Rigid body and torsional behaviour

(%) comparison to the as-built value

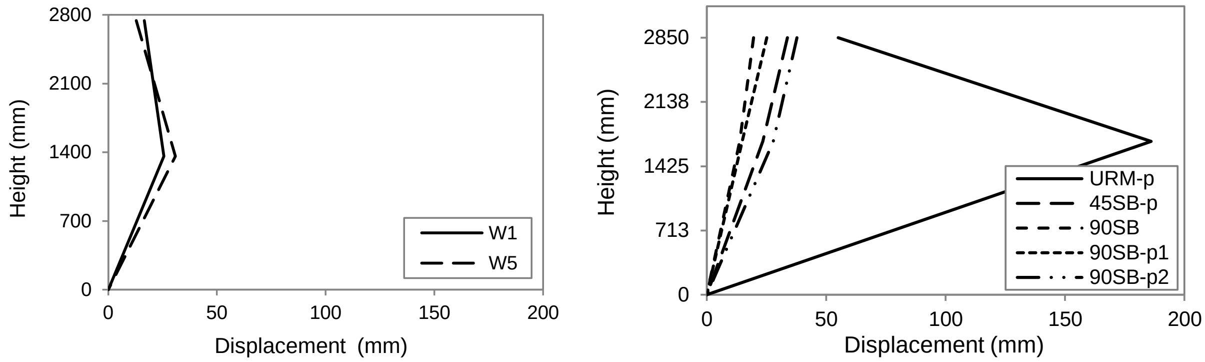

(a) Cavity-walls (b) Solid-walls

Figure 7. Displacement profiles

4 CONCLUSIONS

Shake-table tests were undertaken in order to experimentally validate simple and cost-effective seismic retrofit solutions for clay brick URM cavity- and solid-walls and the following conclusions were drawn:

- The critical failure mode for URM walls in the as-built condition was one-way bending in the out-of-plane direction with crack formation at three quarter-height enabling the wall to act as two separate rocking bodies. In the cavity-walls, bending of the original cavity-ties and subsequent differential movements between masonry leaves was observed.
- All of the tested retrofitted walls sustained increased PGA values with reduced lateral displacements experienced up the height of the wall. The most effective mitigation system was the use of 90 x 45 mm timber strong-backs from wall base to parapet top, which allowed flexural behaviour with a significant reduction in displacement and an increased PGA of three times the as-built condition for both cavity- and solid-walls.
- The use of 90 x 90 mm timber strong-backs further decreased the lateral displacement experienced, resulting in rigid-body behaviour. The parapet failure induced earlier instability with respect to the dynamic loading sustained by 45SB-p.
- Timber strong-backs were the most cost-effective and simple to install securing technique implemented. Standard 90 x 45 mm timber framing can be used as strong-backs, and do not require a specialist construction contractor to install.

- The roof diaphragm interaction with the wall provided a weak plane for cracking to form and the parapet to fail.
- Mechanical screw ties provided adequate wall-to-roof diaphragm connection during dynamic loading. Brick pull-out was observed prior to screw pull-out from bricks.

5 ACKNOWLEDGMENTS

The authors wish to thank the Building Research Association of New Zealand (BRANZ), the New Zealand Natural Hazards Research Platform and the QuakeCoRe Centre for Earthquake Resilience for funding the experimental campaigns. The efforts of students at the University of Auckland are gratefully acknowledged, including Chengliang (Liang) Qian, Xi (Kevin) Jiang, Kevin Crowe, Timothy Cleaver, and Sean Bissett. The authors are also thankful to ITW New Zealand for proving components for the test frame and to Steel Stuff Limited for proving fabrication assistance.

6 REFERENCES

ASTM. (2013). C109 - Standard Test Method for Compressive Strength of Hydraulic Cement Mortars ASTM International. Pennsylvania, United States.

ASTM. (2016a). C67 - Standard Test Methods for Sampling and Testing Brick and Structural Clay Tile. ASTM International. Pennsylvania, United States.

ASTM. (2016b). C1314 - Standard Test Method for Compressive Strength of Masonry Prisms. ASTM International. Pennsylvania, United States.

Dizhur, D. & M. Griffith, et al. (2014). "Out-of-plane strengthening of unreinforced masonry walls using near surface mounted fibre reinforced polymer strips." Engineering Structures **59**(0): 330-343.

FEMA (2006). FEMA 547/2006 Techniques for the Seismic Rehabilitation of Existing Buildings. United States of America: FEMA.

Giaretton, M. & Dizhur, D. et al. (2016a). "Construction Details and Observed Earthquake Performance of Unreinforced Clay Brick Masonry Cavity-walls." Structures **6**: 159-169.

Giaretton, M. & Dizhur, D. et al. (2016b). "Shaking table testing of as-built and retrofitted clay brick URM cavity-walls." Engineering Structures **125**: 70-79.

King, K.W., Wawclawczyk, J. H. & Ozbey, C. (2009). "Retrofit strategies to protect structures from blast loading " Canadian Journal of Civil Engineering **36**(8): 1345-1355.

Meisl, C., Elwood, K. & Ventura, C. (2007). "Shake table tests on the out-of-plane response of unreinforced masonry walls." Canadian Journal of Civil Engineering **34**(11): 1381-1392.

Penner, O. & K.J. Elwood (2016). "Out-of-Plane Dynamic Stability of Unreinforced Masonry Walls in One-Way Bending: Shake Table Testing." Earthquake Spectra **32**(3): 1675-1697.

Ruggieri, N., Tampone, G. & Zinno, R. (2015). Historical earthquake-resistant timber frames in the Mediterranean area.

Russell, A. (2010). Seismic Assessment of In-Plane Unreinforced Masonry Walls. Department of Civil and Environmental Engineering Auckland, University of Auckland. **PhD**.

Russell, A.P. & Ingham, J.M. (2010). "Prevalence of New Zealand's unreinforced masonry buildings." Bulletin of the New Zealand Society for Earthquake Engineering **43**(3): 182-201.

Tsakanika-Theohari, E. (2008). "The constructional analysis of timber load bearing systems as a tool for interpreting Aegean Bronze Age architecture." Bronze Age Architectural Traditions in the Eastern Mediterranean. Diffusion and Diversity **7**(8): 127-142.

Walsh, K.Q., Dizhur, D.Y. et al. (2015). "In Situ Out-of-Plane Testing of Unreinforced Masonry Cavity Walls in as-Built and Improved Conditions." Structures **3**: 187-199.